Published in final edited form as:
Mol Pharm. 2011 October 3; 8(5): 1662–1668. doi:10.1021/mp100466m.

Uptake and intracellular fate of multifunctional nanoparticles: a comparison between lipoplexes and polyplexes via quantum dots-FRET

Yun Wu[1], **Yi-Ping Ho**[2], **Yicheng Mao**[1], **Xinmei Wang**[1], **Bo Yu**[1], **Kam W. Leong**[2], and **L. James Lee**[1,3,*]

[1]Nanoscale Science and Engineering Center for Affordable Nanoengineering of Polymeric Biomedical Devices, The Ohio State University, 174 W 18th Avenue, Columbus, OH 43210

[2]Department of Biomedical Engineering, Duke University, CIEMAS 1395, PO Box 90281, Durham, NC 27708

[3]William G. Lowrie Department of Chemical and Biomolecular Engineering, The Ohio State University, 140 West 19th Avenue, Columbus, OH 43210

Abstract

Lipoplexes and polyplexes represent the two major nanocarrier systems for nucleic acid delivery. Previous studies examining their uptake and intracellular unpacking rely on organic fluorophores fraught with low signal intensity and photobleaching. In this work quantum dots-mediated Förster resonance energy transfer (QD-FRET) was first used to study and compare the cellular uptake and the intracellular fate of oligodeoxynucelotide (ODN)-based lipoplexes and polyplexes. QD605-Amine and Cy5-labeled ODN (Cy5-GTI2040) were chosen as the FRET pair. By adjusting the lipids/ODN ratio of lipoplexes and the nitrogen/phosphate (N/P) ratio of polyplexes, lipoplexes and polyplexes with comparable physical properties were produced. The biological activities of dual-labeled lipoplexes and polyplexes remained unaltered compared to their unlabeled counterparts as evidenced by their comparable antisense activities against protein R2 in KB cells. Flow cytometry and confocal microscopy revealed similar pattern of uptake for these two types of nanoparticles, although polyplexes had a higher dissociation rate than lipoplexes in KB cells. We demonstrate that QD-FRET is a sensitive tool to study the uptake and intracellular unpacking of lipoplexes and polyplexes, which may help optimize their formulations for various theranostics applications.

Keywords

quantum dots; FRET; lipoplexes; polyplexes; multifunctional nanoparticles; oligodeoxynucleotide (ODN); KB cells

Introduction

Nanomedicine, coined for the application of nanotechnology to medicine, shows great potential to impact healthcare [1]. The use of nanocarriers to deliver nucleic acid-based therapeutics is particularly promising for the advance of molecular and genetic medicine [2–5].

*To whom correspondence should be addressed. lee.31@osu.edu.

Supporting Information
This material is available free of charge via the Internet at http://pubs.acs.org.

Among them, lipoplexes and polyplexes represent the two major non-viral nanocarrier systems most widely studied [2–5]. Lipoplexes use cationic lipids to encapsulate nucleic acids, while polyplexes rely on cationic polymers to condense nucleic acids, forming nanocomplexes. To achieve multi-functionality, these nanocomplexes can be tagged with labels such as iron oxide nanoparticles for in vivo MRI, gold nanoparticles for photothermal treatment, or quantum dots (QDs) for optical imaging [6–10]. Quantum dots enjoy high quantum yield, narrow photoluminescence spectra and high photostability [10], rendering them particularly attractive for theranostic applications [11, 12]. They can also serve as efficient electron donors in FRET-based biophotonics.

Förster resonance energy transfer (FRET) is a useful tool in evaluating molecular dynamics at the nanometer scale [13, 14]. Organic fluorescence dyes, such as fluorescein and rhodamine or Cy3 have been used as energy donor and energy receptor, respectively, to study the stability and intracellular fate of lipoplexes and polyplexes [13, 14]. Compared with conventional FRET, quantum dots-mediated FRET (QD-FRET) overcomes the disadvantages such as spectral crosstalk, photobleaching and direct acceptor excitation because of the unique photo physical properties of QDs [15–19]. In a recent review, Medintz et al. (2009) summarized the applications of QD-FRET in sensing DNA, protein, antibody, enzymatic activity, pH and ion concentration changes during biological processes [15]. In the context of gene delivery, QD-FRET is particularly useful for evaluating the dissociation of the DNA nanocomplexes, one of the major barriers in nonviral gene transfer [20]. For instance, our group has applied QD-FRET to study the intracellular fate of pDNA/polycation complexes and compared the unpacking kinetics among chitosan, polyethylenimine and polyphosphoramidate [17–19]. Recently Lee et al. (2010) investigated the intracellular trafficking of siRNA/QD-polyethylenimine (PEI) complexes [16]. Although QDs have been encapsulated in lipoplexes previously to form multifunctional nanoparticles for cancer treatment [21, 22], little research has been done to evaluate the uptake and their intracellular fate via QD-FRET.

In this study, QD-FRET was integrated with nucleic acid-loaded delivery vehicles, forming multifunctional (therapeutic and imaging) nanoparticles. As shown in Figure 1, QD605-Amine and Cy5 labeled oligodeoxynucelotides (ODN, Cy5-GTI2040) were chosen as the FRET pair and encapsulated in lipoplexes. Upon excitation at 405nm, the QD-FRET mediated Cy5 emission indicates compact and intact lipoplexes, while the disappearance of QD-FRET mediated Cy5 emission suggests the dissociation of lipoplexes. This work presented the first demonstration of using QD-FRET to study the intracellular stability of lipoplexes. We also compared the uptake and intracellular fate between lipoplexes and polyplexes, and demonstrated that QD-FRET is a universal and sensitive tool that may help better design multifunctional nanoparticles for nanomedicine.

Materials and methods

Materials

QD605-Amine was purchased from eBioscience, Inc. (93-6366-33). The Cy5 labeled phosphorothioate oligodeoxynucleotide (Cy5-GTI2040, 5′-Cy5-TCT CCC AGC GTG CGC CAT-3′) were custom synthesized by Alpha DNA, Inc. (Montreal, Canada). 2, 3-Dioleoyloxy-propyl-trimentylammoniumchlorid (DOTAP) was purchased from Genzyme Inc. (LP-04-117). Egg phosphatidylcholine (Egg PC) and methoxy-polyethylene glycol (MW≈2,000Da)-distearoyl phosphatidyl- ethanolamine (PEG-DSPE) were obtained from Lipoid (Newark, NJ). Polyethylenimine (PEI, Branched, 25KDa, Sigma Aldrich, St. Louis, MO) was obtained from Sigma. 200 proof ethanol was purchased from Pharmco-Aaper (E200GP). 1X PBS was purchased from Fisher Scientific (14190-136).

Preparation of QD605-Amine and Cy5-GTI2040 encapsulated lipoplexes (QD605/Cy5-GTI2040 lipoplexes) via ethanol dilution method

QD605-Amine and Cy5-GTI2040 were first mixed at equal volume and incubated at room temperature for 1 hr protected from light. The lipid mixture in ethanol (DOTAP: EggPC: PEG-DSPE= 30:69:1 molar ratio) was then added into the QD605-Amine and Cy5-GTI2040 mixture to achieve 40% ethanol and 60% aqueous in the final mixture with the lipids to Cy5-GTI2040 mass ratio of 12.5. The mixture was then dialyzed against 1X PBS buffer overnight to remove ethanol and QD605/Cy5-GTI2040 lipoplexes were thus formed.

Preparation of QD605-PEI and Cy5-GTI2040 polyplexes (QD605/Cy5-GTI2040 polyplexes)

PEI was labeled with QD605-Amine according to the manufacturer's protocol. Briefly, QD605-Amine were activated by bis(sulfosuccinimidyl) suberate (BS3, Thermo Fisher Scientific, Rockford, IL) in 1X Borate buffer (50 mM, pH 8.5, Thermo Fisher Scientific, Rockford, IL) for 30 min at room temperature. The reactive QD605-Amine were then purified and concentrated by PD-10 desalting column (GE Healthcare Biosciences, Piscataway, NJ) and ultrafiltration unit (100 kDa cutoff, Amicon Ultra-4 centrifugal filter units, Millipore, Billerica, MA), respectively. To facilitate complete conjugation of QD605-Amine, the molar ratio of QD605-Amine to PEI was kept at 1:4. The QD605-PEI conjugate was then purified by ultrafiltration with 100 kDa cutoff and resuspended in 1X borate buffer.

The synthesis of QD605-PEI and Cy5-GTI2040 polyplexes has been described elsewhere [23]. Briefly, Cy5-GTI2040 and QD605-PEI were dissolved in 10 mM sterile HEPES solutions (pH 7.2). Complexes were formed by adding equal volumes of QD605-PEI solution to the Cy5-GTI2040 solution and then vigorously mixing by pipetting or brief vortexing. The nitrogen/phosphate (N/P) ratio used for polyplexes was 4:1. QD605/Cy5-GTI2040 polyplexes were then used without further purification.

Size and Zeta Potential Measurement

Size and zeta potential were measured by Zetasizer NanoZS-90 (Malvern Instruments, Southborough, MA). Lipoplexes and polyplexes were diluted in an ultra-micro cuvette (BrandTech Scientific, Essex, CT) to a final Cy5-GTI2040 concentration of 10 μg/mL for size measurements. Three measurements, each consisting of twelve 10 sec runs, were performed at 25 °C at 90° scattering angle. The size stability of QD605/Cy5-GTI2040 lipoplexes and polyplexes was monitored for 6 h (measured every 5 min) in 10% fetal bovine serum (FBS, Gbico 160000) in PBS. Z average diameter, derived from a Cumulants analysis of the measured correlation curve, was reported as the intensity weighted mean hydrodynamic radius. Reported polydispersity index (PDI) width (σ) in the size measurement assumed a Gaussian distribution and was defined in the fashion of $\sigma^2 = PDI \times (Z_{Ave})^2$ (Malvern Instrument Manual). Zeta potential measurements were performed at a final Cy5-GTI2040 concentration of 2 μg/mL using a capillary flow cell (Malvern Instruments, Southborough, MA) at 25 °C. Smoluchowski model was used to calculate the zeta potential obtained from five measurements, each consisting of twelve runs.

Fluorospectrophotometry

QD605/Cy5-GTI2040 lipoplexes and polyplexes were diluted to a final Cy5-GTI2040 concentration of 2 μg/mL in a plastic methacrylate cuvette (Fisher Scientific, Pittsburg, PA). Fluorescence emission spectra (550–750 nm) of lipoplexes and polyplexes upon excitation at 488 nm were scanned by a spectrofluorometer (Cary Eclipse, Varian, Palo Alto, CA).

KB Cell Culture

KB cells (human oral carcinoma cell line, a subline of HeLa), obtained from the American type Culture Collection (ATCC) (Manassas, VA), were routinely cultured in a 75 cm^2 T flask containing 15 mL of RPMI 1640 media supplemented with 10% FBS. The cells were seeded into 75 cm^2 T flasks at a concentration of 1×10^5 viable cells/mL and incubated at 37°C in a humidified atmosphere containing 5% CO_2. The cells were subcultured every 3 days.

Transfection studies of QD605/Cy5-GTI2040 lipoplexes and polyplexes

KB cells were seeded at 2×10^5 viable cells/well in 6 well plates containing 2 mL of culture medium supplemented with 10% FBS, or at 4×10^4 viable cells/well on cover glasses (Fisher Scientific, 12-545-82) in 24 well plates containing 0.4 mL of culture medium supplemented with 10% FBS. The cells were incubated at 37 °C in a humidified atmosphere containing 5% CO_2 overnight. Then the culture medium was replaced with the medium containing no FBS. QD605/Cy5-GTI2040 lipoplexes and polyplexes were then added into the medium at the Cy5-GTI2040 concentration level of 1 uM. The cells were incubated at 37 °C for 4 hours, and the transfection process was stopped by transferring cells into fresh culture medium supplemented with 10% FBS (2mL for 6 well plates and 0.4mL for 24 well plates). All transfection experiments were performed in triplicate.

Cytotoxicity of lipoplexes and polyplexes

The cytotoxicity of lipoplexes and polyplexes was evaluated using alamarBlue® assay (Invitrogen, A13262). 48 h post transfection, the cells were incubated with fresh culture medium containing 10% alamarBlue for 2 h at 37 °C in a humidified, 5% CO_2 atmosphere, protected from light. The fluorescence intensity was read at an emission wavelength of 590 nm under the excitation wavelength of 570 nm using a microplate reader (GENios Pro, Tecan, USA).

Quantification of R2 mRNA expression in KB Cells by quantitative real time PCR (qRT-PCR)

48 h post transfection, the cells were washed with cold 1X PBS twice and then treated with 1 mL TRIzol (Invitrogen). Total RNA was extracted by adding chloroform. The total RNA was further purified by isopropanol precipitation and washed by 70% ethanol. The total RNA was transcribed into cDNA using the first-strand cDNA synthesis kit (Invitrogen 18080051). The resulting cDNA was amplified by qRT-PCR (Taqman Assay Hs01072067_gl). Relative gene expression values were determined by the ΔΔCT method. R2 expression was normalized to 18S, which was the endogenous reference in the corresponding samples, and relative to the untreated control cells.

Uptake and intracellular fate of QD605/Cy5-GTI2040 lipoplexes and polyplexes in KB cells

The cellular uptake and intracellular fate of the QD605/Cy5-GTI2040 lipoplexes and polyplexes were examined by flow cytometry (BD LSR II, San Jose, CA, USA) and laser scanning confocal microscopy (Olympus FV1000, Center Valley, PA, USA). In flow cytometry experiments, KB cells were cultured in 6 well plates and transfected with QD605/Cy5-GTI2040 lipoplexes or polyplexes following the aforementioned transfection procedure. The cells were harvested 0.5, 1, 2 and 4 h after the addition of lipoplexes or polyplexes. For the rest of the samples, the transfection process was stopped 4 h after the cells were incubated with nanoparticles by transferring the cells into 2 mL fresh culture medium supplemented with 10% FBS. The rest samples were harvested 24, 48 and 72 h post transfection. To harvest the samples, the cells were first detached from culture plates using 0.25% trypsin, washed with PBS twice and fixed using 4% paraformaldehyde. The

fluorescence signals of QD605 and FRET-mediated Cy5 were observed in the QD605 and PE-Cy5 channels respectively. 100000 events were collected for each sample and the average results of 3 replicates were reported.

In confocal microscopy experiments, KB cells were cultured on cover glasses in 24 well plates and treated with QD605/Cy5-GTI2040 lipoplexes or polyplexes following the aforementioned transfection procedure. Cells were harvested 0.5, 1, 2 and 4 h after the addition of nanoparticles. For the rest of the samples, after the cells were incubated with nanoparticles for 4 h, the transfection process was stopped by transferring the cells into 0.4 mL fresh culture medium supplemented with 10% FBS. The rest of the samples were harvested 24 and 48 h post transfection. To harvest the samples, cells were washed with 1X PBS twice and fixed with 4% paraformaldehyde at room temperature for 1 h. The cells were then washed with PBS twice and mounted on glass slides for confocal microscopy analysis. The excitation wavelength was set at 405 nm and the fluorescence signals of QD605 and Cy5-GTI2040 were observed in the QD605 (dichroic mirror 560–620nm) and Cy5 (dichroic mirror 655–755nm) channels respectively.

Results and discussion

Size and surface charge of QD605/Cy5-GTI2040 lipoplexes and polyplexes

Figure 2 shows the size and zeta potential of QD605/Cy5-GTI2040 lipoplexes and polyplexes. The mean diameter of the lipoplexes is 141±2 nm and polyplexes is 169±6 nm. Standard deviations reported herein were obtained from three separate measurements. The zeta potential of lipoplexes is 6.93±0.83 mV and polyplexes is 13.24±3.62 mV. At the lipids/ODN ratio of 12.5 for lipoplexes and the N/P ratio of 4 for polyplexes, these two types of nanoparticles had comparable size, and polyplexes had higher positive surface charges than lipoplexes. A summary of size and zeta potential of other lipoplexes and polyplexes used in this work were provided in the Supporting Information (Table 1s). The sizes of lipoplexes and polyplexes were also monitored in 10% FBS in PBS (mimicking the regular culture condition) for a 6-hour period. Both lipoplexes and polyplexes exhibited good stability (Figure 1s in Supporting Information).

FRET of QD605/Cy5-GTI2040 lipoplexes and polyplexes

The FRET of QD605/Cy5-GTI2040 lipoplexes and polyplexes was investigated with fluorospectrophotometer. Figure 3 shows the normalized fluorospectra of lipoplexes and polyplexes excited at 488 nm. The emission at 670 nm of Cy5-GTI2040 demonstrated that QD605 and Cy5-GTI2040 were successfully encapsulated inside lipoplexes, and QD605-PEI successfully conjugated with Cy5-GTI2040 to form polyplexes. Energy transfer was evaluated by the ratio of acceptor to donor (I_{Cy5}/I_{QD605}), calculating the area under the curve of the acceptor emission (630–750 nm) and the donor emission (550–629 nm). For polyplexes, Cy5-GTI2040 was condensed by QD605-PEI, bringing energy donor and acceptor into proximity. For lipoplexes, QD605 and Cy5-GTI2040 were encapsulated inside lipid bilayers, and Cy5 associated not only with QD605 but also with cationic lipids. It is thus suspected that the QD605 stay closer to Cy5 within polyplexes than lipoplexes (I_{Cy5}/I_{QD605}=1.27), rendering higher energy transfer efficiency for polyplexes (I_{Cy5}/I_{QD605}=2.71).

Cytotoxicity of lipoplexes and polyplexes

The cytotoxicity of lipoplexes and polyplexes was evaluated in KB cells 48 h post transfection. In addition to QD605/Cy5-GTI2040 lipoplexes and polyplexes, GTI2040 lipoplexes/polyplexes, QD605/GTI2040 lipoplexes/polyplexes and Cy5-GTI2040 lipoplexes/polyplexes were incorporated as controls to evaluate the effects of QD605 and the effects of Cy5 labeling of GTI2040 on the cytotoxicity of both nanoparticles. As shown

in Figure 4, compared with untreated cells, little, if any, cytotoxicity was observed with lipoplexes, however, polyplexes exhibited some cytotoxicity caused by PEI. The cytotoxicity of polyplexes can be reduced by reducing the amount of PEI used in the polyplexes, i. e. decreasing the N/P ratios. However, the transfection efficiency may be impaired. In this work, the N/P ratio of 4 was selected by balancing between the cytotoxicity and the transfection efficiency.

Inhibition of R2 gene expression by lipoplexes and polyplexes in KB cells

The bioactivities of QD605/Cy5-GTI2040 lipoplexes and polyplexes were evaluated in KB cells. GTI2040 is a specially designed 20-mer antisense ODN. It can hybridize to the mRNA of the R2 subunit of human ribonucleotide reductase (RNR) and thus inhibit the R2 expression. It has shown potent antitumor activity against a variety of tumors. KB cells were transfected with QD605/Cy5-GTI2040 lipoplexes and polyplexes. In addition, GTI2040 lipoplexes/polyplexes, QD605/GTI2040 lipoplexes/polyplexes and Cy5-GTI2040 lipoplexes/polyplexes were used as controls to investigate the effects of QD605 and the effect of Cy5 labeling of GTI2040 on R2 expression. 48 h post transfection, the down-regulation of R2 target was evaluated at the mRNA level. As shown in Figure 5, all lipoplexes and polyplexes successfully down-regulated the R2 target when cells were treated at Cy5-GTI2040 or GTI2040 concentration level of 1 μM. We observed 64.5±6.2% down-regulation by GTI2040 lipoplexes and 68.2±5.5% by GTI2040 polyplexes; 68.4±9.0% by QD605/GTI2040 lipoplexes and 66.8±9.7% by QD605/GTI2040 polyplexes; 71.3±5.9% by Cy5-GTI2040 lipoplexes and 68.2±6.9% by Cy5-GTI2040 polyplexes; and 59.1±7.0% by QD605/Cy5-GTI2040 lipoplexes and 70.2±6.4% by QD605/Cy5-GTI2040 polyplexes. These results showed that the addition of QD605 did not affect the biological activities of lipoplexes and polyplexes, and the Cy5 labeling had little, if any, effect on the biological function of GTI2040. Both lipoplexes and polyplexes were good delivery systems that had comparable delivery efficiency and provided comparable R2 down-regulation. Our results were consistent with the results of pDNA delivery via lipoplexes and polyplexes by Matsumoto et al. [13].

Cellular uptake and intracellular fate of QD605/Cy5-GTI2040 lipoplexes and polyplexes in KB cells

The cellular uptake and intracellular fate of QD605/Cy5-GTI2040 lipoplexes and polyplexes in KB cells were investigated by laser scanning confocal microscopy and flow cytometry. Lipoplexes and polyplexes exhibited similar intracellular fate. Confocal microscopy images (Figure 4) show the representative cellular uptake and intracellular fate of lipoplexes and polyplexes in the majority of the cells. The fluorescence of QD605 was pseudo colored green in order to distinguish it from the red fluorescence of FRET-mediated Cy5. As shown in Figure 6(a), 0.5 h and 1 h after the addition of lipoplexes and polyplexes, much less fluorescence signal was observed in the cells treated with lipoplexes than those treated with polyplexes, suggesting that cellular uptake of lipoplexes was less significant compared with polyplexes. And for cells treated with polyplexes, the green fluorescence of QD605 and the red fluorescence of FRET-mediated Cy5 were mainly co-localized around the cells, indicating polyplexes mainly accumulated around the cell edge.

The entry of nanoparticles into cells involves the binding of nanoparticles to the cell surface and the internalization, i.e. the uptake, of nanoparticles inside the cells. Polyplexes have higher positive surface charge than lipoplexes. The higher the surface charges are, the stronger the interaction exists between positively charged nanoparticles and negatively charged cell membrane, and this might be one reason that polyplexes showed faster initial cellular uptake than lipoplexes. The uptake of lipoplexes and polyplexes is a complicated process and is not well understood. It is generally agreed that nanoparticles are internalized

by the cells via endocytosis, however, which specific endocytosis pathway, including the clathrin-dependent pathway, the caveolin-dependent pathway, phagocytosis, macropinocytosis, and the clathrin/caveolin independent pathways, is responsible for cellular uptake strongly depends on the cell type [24–26]. In this work, different endocytosis pathways might be involved in the uptake of lipoplexes and polyplexes, which may also lead to different cellular uptake rates.

At 2 h after the addition of lipoplexes and polyplexes, the fluorescence signals of both QD605 and FRET-mediated Cy5 became stronger, indicating more cellular uptake of polyplexes. At this time point, although intracellular lipoplexes could be detected, the majority of the lipoplexes was mainly accumulated around the edge of the cells, while some polyplexes moved from the edge toward the center of the cells. At 4 h after the addition of lipoplexes and polyplexes, maximum green fluorescence of QD605 and red fluorescence of FRET-mediated Cy5 were observed, indicating that lipoplexes and polyplexes were successfully uptaken by the cells, and at this time point the co-localization of QD605 and FRET-mediated Cy5 fluorescent signal suggested that the majority of lipoplexes and polyplexes were still intact and not dissociated. However we did observe some lipoplexes and polyplexes dissociating in some cells, indicating the unpacking of lipoplexes and polyplexes was as early as 4 h after the treatment, which was consistent with the observation by Lee et al. [16] (data not shown). 24 h later, the red fluorescence of FRET-mediated Cy5 decayed in many cells, indicating that more lipoplexes and polyplexes unpacked or degraded, and thus the QD605 dissociated from Cy5-GTI2040, which led to the disappearance of red fluorescence from FRET-mediated Cy5. Exocytosis might also have contributed to the disappearance of the FRET signal. 48 h post transfection, little red fluorescence of FRET-mediated Cy5 but only green fluorescence of QD605 was observed in most cells, indicating that the majority of lipoplexes and polyplexes broke up and the QD605 were not able to excite the Cy5-GTI2040.

Different from conventional pixel-counting methods used in confocal images, flow cytometry analysis was used to confirm the aforementioned observations in a more quantitatively manner. A typical set of flow cytometry results was provided in supporting materials. As shown in Figure 7, from 0.5 h to 4 h after the addition of lipoplexes and polyplexes, the fluorescence signals of QD605 and FRET-mediated Cy5 became stronger and stronger, suggesting that more and more lipoplexes and polyplexes were uptaken by the cells. Compared with lipoplexes and polyplexes, the mixture of free QD605 and free Cy5-GTI2010 showed much weaker fluorescence signals of QD605 and FRET-mediated Cy5, demonstrating that both lipoplexes and polyplexes are good carrier systems for the delivery of QD605 and Cy5-GTI2040. 24 h post transfection, the FRET-mediated Cy5 signal decayed significantly, suggesting the dissociation of lipoplexes and polyplexes, and thus the abrogation of FRET-mediated Cy5 emission, due to the separation of donors and acceptors. The FRET-mediated Cy5 signal of polyplexes started to level off, indicating the unpacking was almost finished 24 h post transfection, which was consistent with the results we observed with the unpacking of pDNA polyplexes [18]. The FRET-mediated Cy5 signal of lipoplexes, however, was further decreased at 48 h and then leveled off 72 h post transfection, indicating that the majority of lipoplexes broke up 48 h post transfection. Comparing polyplexes with lipoplexes, we found that polyplexes had a higher dissociation rate than lipoplexes, which might be due to the different delivery mechanism of the two types of complexes. Polyplexes rely on the proton sponge effect to break up and release the ODN [3, 27], while endosomal escape is known to be a limiting step when using lipoplexes to deliver nucleic acids [28, 29]. For lipoplexes, the cationic lipids of the lipoplexes may interact with the anionic lipids of the endosomal membrane, and ODN is then released into the cytoplasm when the anionic lipids “flip-flop” across the bilayer to form the neutral ion pairs with the cationic lipids of the lipoplexes [28, 29]. Another hypothesis states that ODN may be

released when the positively charged lipoplexes fuses with the negatively charged cell membrane [30]. According to our QD-FRET results, we found that the majority of our lipoplexes entered the cells through endocytosis, which agreed with the first hypothesis and others' work [24, 25], and thus generated a high FRET signal right after transfection. If lipoplexes entered the cells by fusion with cell membrane, then lipoplexes would break up during cellular uptake, and thus no FRET signal should be observed.

Conclusions

Lipoplexes and polyplexes are two major nanocarrier systems widely used to deliver nucleic acid drugs in cancer treatment. It is important to understand their cellular uptake and intracellular fate in order to improve the efficacy of nanoparticles. In this work, we demonstrated that QD-FRET is a sensitive and universal tool to study the cellular uptake and intracellular fate of lipoplexes and polyplexes. QD605 and Cy5-GTI2040 were chosen as the FRET donor-receptor pair. By controlling the lipids/ODN ratio of lipoplexes and the N/P ratio of polyplexes, we produced lipoplexes and polyplexes with comparable physical properties, i.e. comparable size and surface charges. The biological activities of lipoplexes and polyplexes were examined in KB cells. The antisense activities against R2 gene expression were first evaluated to confirm that QD605 and the Cy5 labeling of GTI2040 did not affect the biological activities of lipoplexes and polyplexes. Both lipoplexes and polyplexes are good nanocarrier systems that successfully down-regulated R2 gene expression: 59.1±7.0% by QD605/Cy5-GTI2040 lipoplexes and 70.2±6.4% by QD605/Cy5-GTI2040 polyplexes. Confocal microscopy and flow cytometry were used together to investigate the cellular uptake and the intracellular fate of lipoplexes and polyplexes in KB cells. We found that both lipoplexes and polyplexes are efficient nanocarriers in delivering target ODN into KB cells. Although lipoplexes and polyplexes exhibited similar intracellular fate, polyplexes had higher dissociation rate than lipoplexes.

Many factors affect the cellular uptake and the following unpacking of nanoparticles. For lipoplexes, these factors include lipid composition, the types of lipids and the lipid/ODN ratios. For polyplexes, the N/P ratios and the types of polymers play important roles in controlling the delivery of nucleic acid drugs. We believe that by carefully adjusting these factors, we can achieve better cellular uptake and more controllable breakup of nanoparticles and thus the release of nucleic acid drugs. QD-FRET is a powerful tool to visualize the uptake of nanoparticles and their intracellular fate, which may help in better design the nanoparticles to achieve higher efficacy in cancer treatment.

Supplementary Material

Refer to Web version on PubMed Central for supplementary material.

Acknowledgments

This work was supported by the National Science Foundation under grant No. EEC-0425626 and National Institutes of Health under grant No. HL89764.

References

1. Bawarski WE, Chidlowsky E, Bharali DJ, Mousa SA. Emerging nanopharmaceuticals. Nanomedicine: Nanotechnology, Biology, and Medicine. 2008; 4:273–282.
2. Torchilin VP. Targeted Pharmaceutical Nanocarriers for Cancer Therapy and Imaging. The AAPS Journal. 2007; 9:E128–E147. [PubMed: 17614355]
3. Pack DW, Hoffman AS, Pun S, Stayton PS. Design and development of polymers for gene delivery. Nature Reviews Drug Discovery. 2005; 4:581–593.

4. Hughes GA. Nanostructure-mediated drug delivery. Nanomedicine: Nanotechnology, Biology, and Medicine. 2005; 1:22–30.
5. Duncan R. Polymer conjugates as anticancer nanomedicines. Nature reviews. 2006; 6:688–701.
6. Koo OM, Rubinstein I, Onyuksel H. Role of nanotechnology in targeted drug delivery and imaging: a concise review. Nanomedicine: Nanotechnology, Biology, and Medicine. 2005; 1:193–212.
7. Park K, Lee S, Kang E, Kim K, Choi K, Kwon IC. New generation of multifunctional nanoparticles for cancer imaging and therapy. Adv Funct Mater. 2009; 19:1553–1566.
8. Veiseh O, Gunn JW, Zhang M. Design and fabrication of magnetic nanoparticles for targeted drug delivery and imaging. Adv Drug Deliv Reviews. 2010; 62:284–304.
9. Arvizo R, Bhattacharya R, Mukherjee P. Gold nanoparticles: opportunities and challenges in nanomedicine. Expert Opin Drug Deliv. 2010; 7:753–63. [PubMed: 20408736]
10. Medintz IL, Uyeda HT, Goldman ER, Mattoussi H. Quantum dot bioconjugates for imaging, labelling and sensing. Nature Materials. 2005; 4:435–446.
11. Michalet X, Pinaud FF, Bentolila LA, Tsay JM, Doose S, Li JJ, Sundaresan G, Wu AM, Gambhir SS, Weiss S. Quantum dots for live cells, in Vivo Imaging, and Diagnostics. Science. 2005; 307:538–544. [PubMed: 15681376]
12. Ho YP, Leong KW. Quantum dot-based theranostics. Nanoscale. 2010; 2:60–68. [PubMed: 20648364]
13. Matsumoto Y, Itaka K, Yamasoba T, Kataoka K. Intranuclear fluorescence resonance energy transfer analysis of plasmid DNA decondensation from nonviral gene carriers. J Gene Med. 2009; 11:615–623. [PubMed: 19396931]
14. Itaka K, Harada A, Nakamura K, Kawaguchi H, Kataoka K. Evaluation of fluorescence resonance energy transfer of the stability of nonviral gene delivery vectors under physiological conditions. Biomacromolecules. 2002; 3:841–845. [PubMed: 12099831]
15. Medintz IL, Mattoussi H. Quantum dot-based resonance energy transfer and its growing application in biology. Physical Chemistry Chemical Physics. 2009; 11:17–45. [PubMed: 19081907]
16. Lee H, Kim IK, Park TG. Intracellular trafficking and unpacking of siRNA/Quantum dot-PEI complexes modified with and without cell penetrating peptide: confocal and flow cytometry FRET analysis. Bioconjugate Chemistry. 2010; 21:289–295. [PubMed: 20078095]
17. Ho YP, Chen HH, Leong KW, Wang TH. Evaluating the intracellular stability and unpacking of DNA nanocomplexes by quantum dots-FRET. J Control Release. 2006; 116:83–89. [PubMed: 17081642]
18. Chen HH, Ho YP, Jiang X, Mao HQ, Wang TH, Leong KW. Quantitative comparison of intracellular unpacking kinetics of polyplexes by a model constructed from quantum dot-FRET. Molecular Therapy. 2008; 16:324–332. [PubMed: 18180773]
19. Chen HH, Ho YP, Jiang X, Mao HQ, Wang TH, Leong KW. Simultaneous non-invasive analysis of DNA condensation and stability by two-step QD-FRET. Nano Today. 2009; 4:125–134. [PubMed: 20161048]
20. Grigsby CL, Leong KW. Balancing protection and release of DNA: tools to address a bottleneck of non-viral gene delivery. Journal of the Royal Society Interface. 2010; 7:S67–S82.
21. Al-Jamal WT, Al-Jamal KT, Bomans PH, Frederik PM, Kostarelos K. Functionalized-Quantum-Dot-Liposome hybrids as multifunctional nanoparticles for cancer. Small. 2008; 9:1406–1415. [PubMed: 18711753]
22. Al-Jamal WT, Al-Jamal KT, Tian B, Cakebread A, Halket JM, Kostarelos K. Tumor targeting of functionalized quantum dot-liposome hybrids by intravenous administration. Mol Pharm. 2009; 6:520–530. [PubMed: 19718803]
23. Grayson ACR, Doody AM, Putnam D. Biophysical and structural characterization of polyethylenimine-mediated siRNA delivery in vitro. Pharm Res. 2006; 23:1868–1876. [PubMed: 16845585]
24. Elouahabi A, Ruysschaert JM. Formation and intracellular trafficking of lipoplexes and polyplexes. Molecular Therapy. 2005; 11:336–347. [PubMed: 15727930]
25. Khalil IA, Kogure K, Akita H, Harashima H. Uptake Pathways and Subsequent Intracellular Trafficking in Nonviral Gene Delivery. Pharmacol Rev. 2006; 58:32–45. [PubMed: 16507881]

26. Conner SD, Schmid SL. Regulated portals of entry into the cell. Nature. 2003; 422:37–44. [PubMed: 12621426]
27. Godbey WT, Wu KK, Mikos AG. Poly(ethylenimine) and its role in gene delivery. J Control Release. 1999; 60:149–160. [PubMed: 10425321]
28. Lu JJ, Langer R, Chen J. A Novel Mechanism is Involved in Cationic Lipid-Mediated Functional siRNA Delivery. Mol Pharm. 2009; 6:763–771. [PubMed: 19292453]
29. Xu Y, Szoka F. Mechanism of DNA Release from Cationic Liposome/DNA Complexes Used in Cell Transfection. Biochem. 1996; 35:5616–5623. [PubMed: 8639519]
30. Felgner PL, Ringold GM. Cationic Liposome-Mediated Transfection. Nature. 1989; 337:387–388. [PubMed: 2463491]

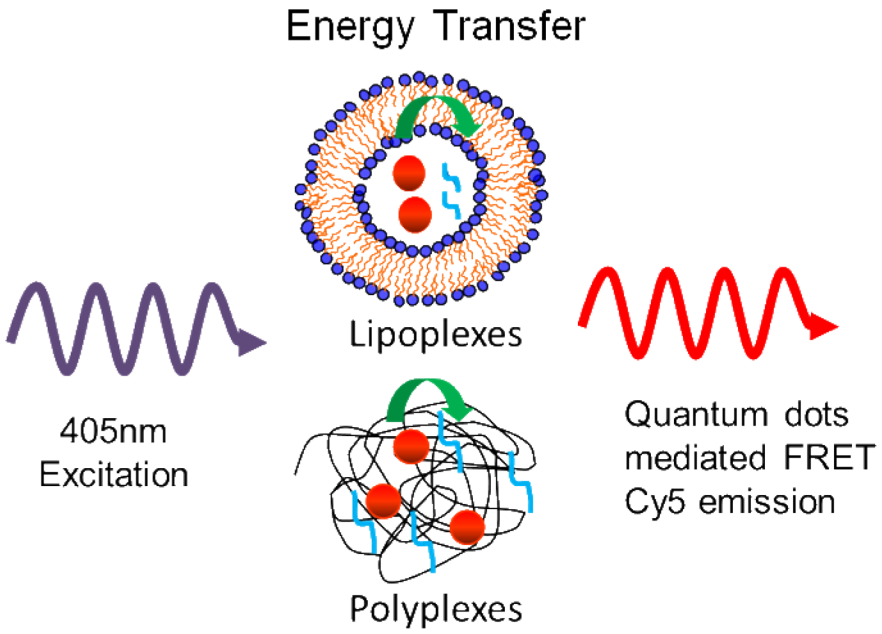

Figure 1.
QD605 and Cy5-GTI2040 were encapsulated in lipoplexes. Cy5-GTI2040 formed polyplexes with QD605-PEI conjugates. Upon excitation at 405nm, the emission of QD-FRET mediated Cy5 indicates compact and intact nanocomplexes.

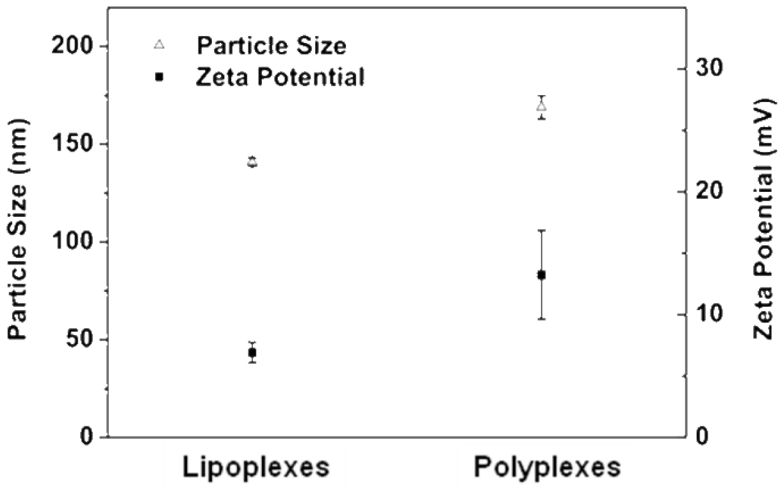

Figure 2.
Size and zeta potential of QD605/Cy5-GTI2040 lipoplexes and polyplexes (n=3).

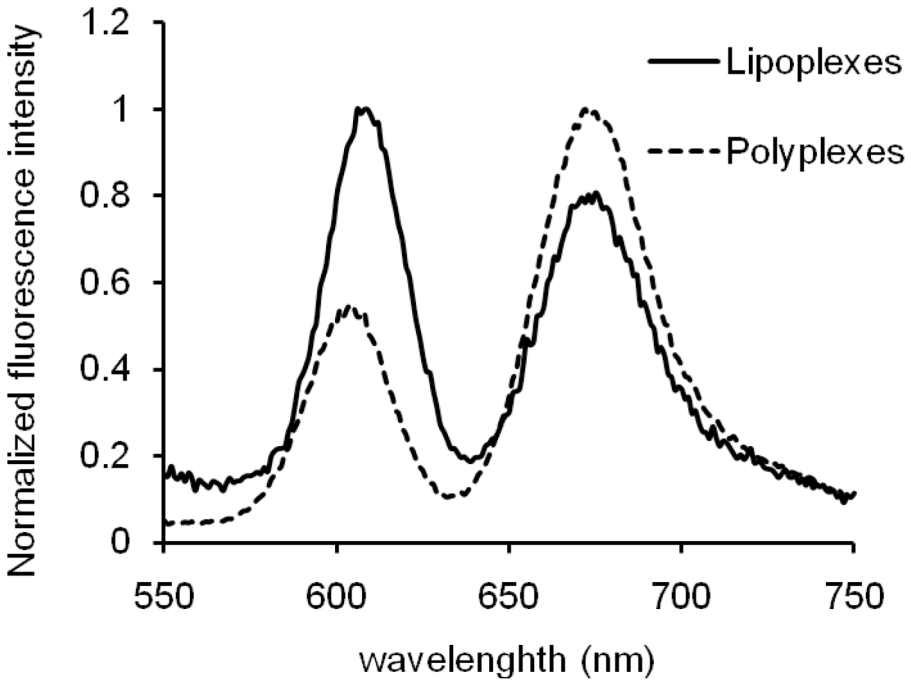

Figure 3.
Fluorospectra of QD605/Cy5-GTI2040 lipoplexes and polyplexes excited at 488nm.

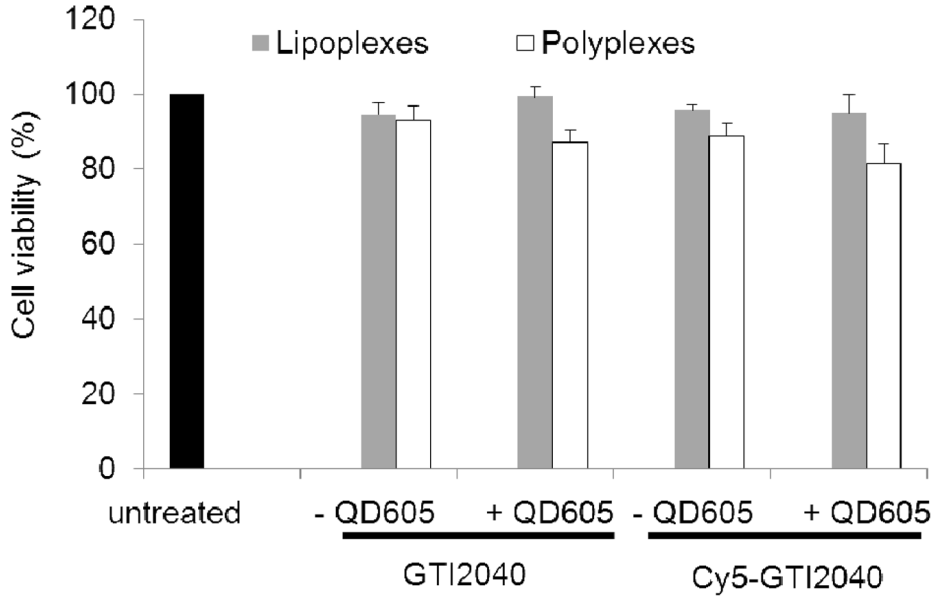

Figure 4.
Cytotoxicity of QD605/Cy5-GTI2040 lipoplexes/polyplexes and their unlabelled counterparts evaluated in KB cells. (n=3)

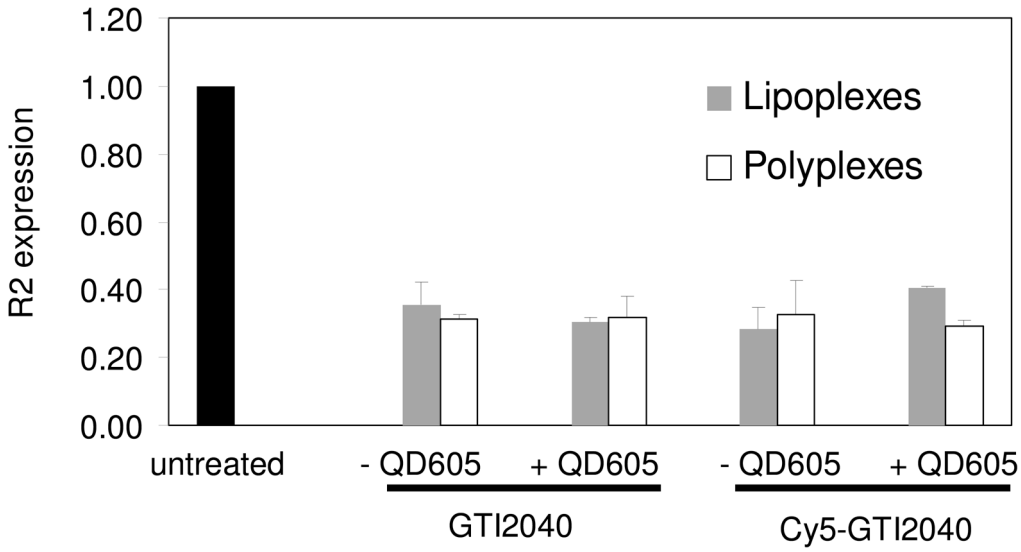

Figure 5.
Inhibition of R2 gene expression in KB cells by lipoplexes and polyplexes compared with untreated control (n=3). No significant difference was found among lipoplexes and polyplexes.

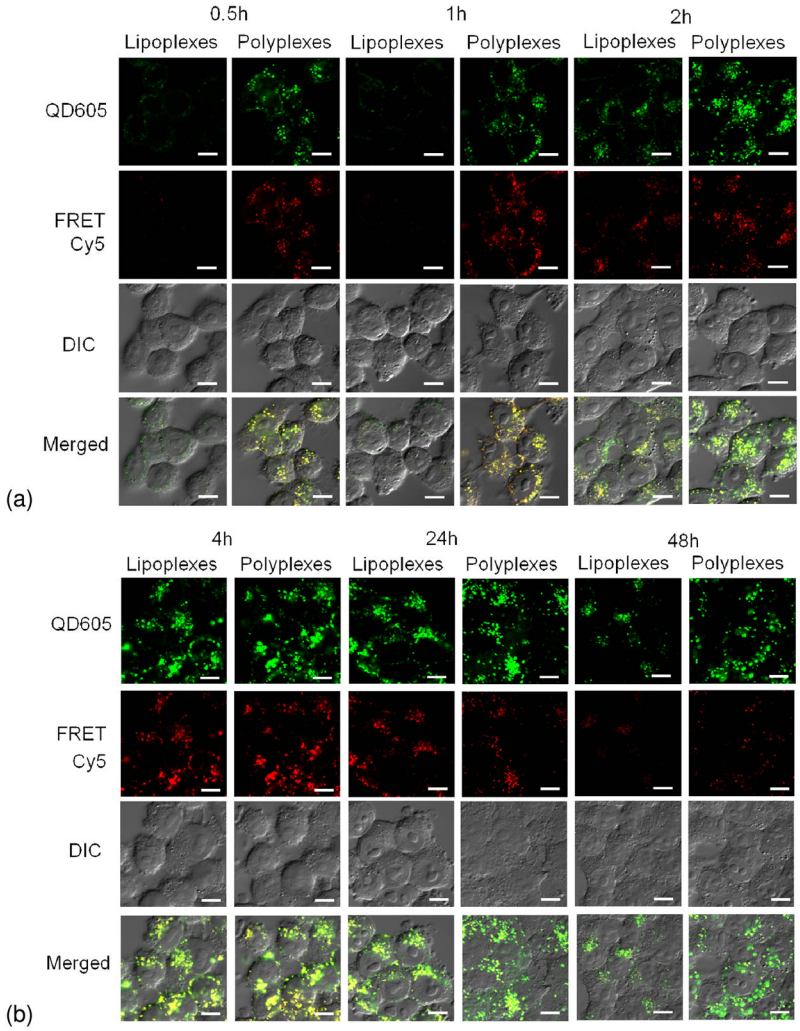

Figure 6.

Cellular uptake and intracellular fate of QD605/Cy5-GTI2040 lipoplexes and polyplexes via confocal microscopy. 0.5 h and 1 h after the addition of lipoplexes and polyplexes, cellular uptake of lipoplexes was less significant than polyplexes. At 2 h, intracellular lipoplexes were detected and more cellular uptake of polyplexes was observed. 4 h later, maximum internalization of lipoplexes and polyplexes was observed, and the co-localization of QD605 and FRET-mediated Cy5 fluorescent signal suggested that the majority of lipoplexes and polyplexes were still intact and not dissociated. At 24 h, lipoplexes and polyplexes unpacked or degraded, and thus the FRET-mediated Cy5 signal decreased. 48 h post transfection, majority of lipoplexes and polyplexes broke up and little FRET-mediated Cy5 signal was detected. (DIC: differential interference contrast. Scale bar: 10um.)

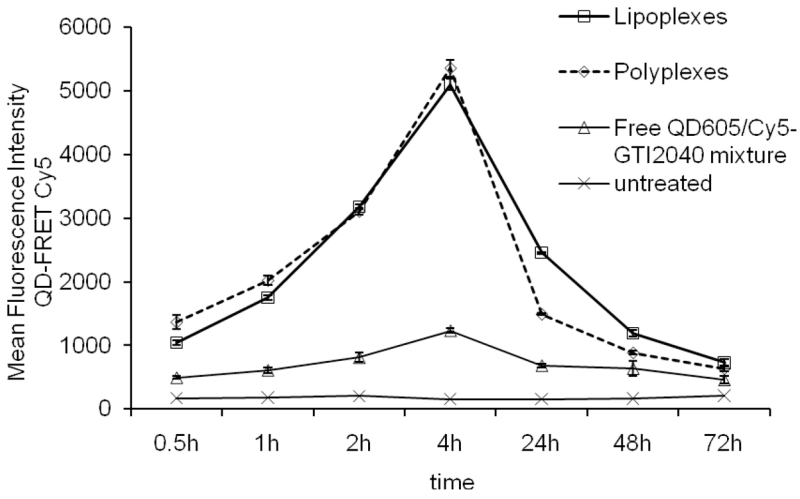

Figure 7.

Cellular uptake and intracellular fate of QD605/Cy5-GTI2040 lipoplexes and polyplexes via flow cytometry analysis. Mean fluorescence intensity of FRET-mediated Cy5 0.5, 1, 2, 4, 24, 48 and 72 h after the cells were treated with lipoplexes and polyplexes at Cy5-GTI2040 concentration of 1 μM. (n=3). From 0.5 h to 4 h after the addition of lipoplexes and polyplexes, more and more lipoplexes and polyplexes were uptaken by the cells. At 24 h, the decay of FRET-mediated Cy5 signal suggested the dissociation of lipoplexes and polyplexes. Then the FRET-mediated Cy5 signal of polyplexes started to level off, indicating the unpacking of polyplexes was almost finished. The FRET-mediated Cy5 signal of lipoplexes, however, was further decreased at 48 h and then leveled off at 72 h, indicating that the majority of lipoplexes broke up 48 h post transfection.